CSIRO PUBLISHING
www.publish.csiro.au/journals/fpb *Functional Plant Biology*, 2009, **36**, 874–879

3D monitoring spatio–temporal effects of herbicide on a whole plant using combined range and chlorophyll *a* fluorescence imaging

Atsumi Konishi[A,B], *Akira Eguchi*[A], *Fumiki Hosoi*[A] *and Kenji Omasa*[A,C]

[A]Graduate School of Agricultural and Life Sciences, The University of Tokyo, Yayoi 1-1-1, Bunkyo-ku, Tokyo 113-8657, Japan.
[B]Present address: Marine Farm, Yanmar Co., Ltd, 3286 Itoharu, Musashi-machi, Kunisaki-city, Oita 873-0421, Japan.
[C]Corresponding author. Email: aomasa@mail.ecc.u-tokyo.ac.jp

This paper originates from a presentation at the 1st International Plant Phenomics Symposium, Canberra, Australia, April 2009.

Abstract. Spatio–temporal effects of herbicide including 3-(3,4 dichlorophenyl)-1,1-dimethylurea (DCMU) on a whole melon (*Cucumis melo* L.) plant were three-dimensionally monitored using combined range and chlorophyll *a* fluorescence imaging. The herbicide was treated to soil in a pot and the changes in chlorophyll *a* fluorescence images of the plant were captured over time. The time series of chlorophyll fluorescence images were combined with 3D polygon model of the whole plant taken by a high-resolution portable scanning lidar. From the produced 3D chlorophyll fluorescence model, it was observed that the increase of chlorophyll fluorescence appeared along veins of leaves and gradually expanded to mesophylls. In addition, it was found by detailed analysis of the images that the invisible herbicide injury on the mature leaves occurred earlier and more severely than on the young and old leaves. The distance from veins, whole leaf area and leaf inclination influenced the extent of the injury within the leaves. These results indicated difference in uptake of herbicide in the plant from soil depends on structural parameters of leaves and the microenvironments as well as leaf age. The findings showed that 3D monitoring using combined range and chlorophyll *a* fluorescence imaging can be utilised for understanding spatio-temporal changes of herbicide effects on a whole plant.

Additional keywords: herbicide uptake, spatio-temporal change, three-dimensional imaging.

Introduction

Imaging techniques have been widely used for plant function analysis from cells to whole plants (e.g. Omasa 1990; Govindjee and Nedbal 2000; Häder 2000; Omasa *et al*. 2002; Jones and Morison 2007). Two-dimensional (2D) imaging techniques such as multispectral and hyperspectral imaging, thermal imaging, and fluorescence imaging allow non-destructive detection of photosynthesis, transpiration, stomatal response, and substances in leaves. Digital imaging of chlorophyll fluorescence quenching is one of the leading methods used to assess photosynthetic activities in leaves (e.g. Omasa *et al*. 1987; Daley *et al*. 1989; Genty and Meyer 1995; Oxborough 2004) and at cellular levels (e.g. Oxborough and Baker 1997). Combined chlorophyll fluorescence and thermal imaging is useful for analysis of relationships between photochemical and non-photochemical quenching and stomatal response (e.g. Chaerle *et al*. 2003; Omasa and Takayama 2003).

Three-dimensional (3D) structure of plants has a great influence on plant functioning and the microenvironments (Ross 1981; Jones 1983; Campbell and Norman 1989). For example, leaf temperature and microenvironments such as light intensity, air current, air temperature, humidity, and CO_2 concentration differ three-dimensionally in each site surrounding/inside the leaves of a whole plant. The leaf position and distance from leaf veins affect water status and stomatal aperture. Moreover, the stomata change size and aperture depending to cell age and physiological conditions in each leaf site. Consequently, the fluxes of water vapour and carbon dioxide (CO_2) through the boundary layer and stomata vary with each leaf site. And, it plays an important role in sustaining plant functioning such as transpiration and photosynthesis.

Two-dimensional imaging techniques are useful for plant function analysis. However, they are still not enough to investigate relationships between 3D structure and plant functioning. Three-dimensional imaging of *in situ* leaves, tissues and cells improve our understanding of plant function and response to environmental stimuli (Häder 2000; Schurr *et al*. 2006; Omasa *et al.* 2007). Concerning chlorophyll fluorescence imaging for photosynthesis analysis, 3D surface microscopy (Rolfe and Scholes 2002; Endo and Omasa 2007) and

 10.1071/FP09108 1445-4408/09/110874

confocal laser scanning microscopy (Omasa *et al*. 2009) have been developed. For whole plant analysis, we have recently developed a new 3D imaging system, combining 3D range lidar and chlorophyll fluorescence imaging (Omasa *et al*. 2007). In present study, we have therefore applied this system to 3D monitoring and analysis of spatio–temporal effects of herbicide added to soil of a whole plant.

Materials and methods

Plant material

Melon (*Cucumis melo* L.) seedlings were grown in pots (10 cm diameter, 10 cm high) in a growth chamber for ~4 weeks after germination. The plants were illuminated for 12 h each day with fluorescent lights at photosynthesis photon flux (PPF) of 200 μmol m^{-2} s^{-1}. Air temperature was 26.5°C during the day and 24°C at night. Relative humidity was 70% during the day and 90% at night. The pots were filled with artificial soil (mixture of vermiculite and perlite, 2 : 1, v/v). Plants were watered daily with a nutrient solution (1 : 1000 dilution of HYPONeX, HYPONeX Japan Corp., Japan).

Herbicide treatment

The herbicide Nekosogi-ace (Rainbow Chemical, Co., Ltd, Japan), containing 6.0% 3-(3,4 dichlorophenyl)-1,1-dimethylurea (DCMU) was used in the experiment. The herbicide of 10 g L^{-1} (water solubility of DCMU at 25°C is 0.18 mM) dissolved in water was treated to the plant soil in the pot before chlorophyll fluorescence imaging. The concentration was within normal use in the field.

Combined range and chlorophyll fluorescence imaging system

Figure 1 shows (*a*) a combined range and (*b*) chlorophyll *a* fluorescence imaging system. In Fig. 1*a*, a high-resolution portable scanning lidar (modified type of TDS-130 L, Pulstec Industrial Co., Ltd, Japan) was used for the 3D range imaging of a whole plant. The lidar is based on the light-probe method (trigonometry), and is able to obtain 3D point cloud range data of the plant. The accuracy of range measurement was 0.5 mm at a distance of 3.5 m. The spatial resolution was 1.7 mm to *y*-axis and 1.2 mm to *x*-axis. In Fig. 1*b*, a metal halide lamp equipped with a short pass heat absorbing filter (LS-M180, Sumita Optical Glass, Inc., Japan) was used as actinic light of the wavelength from 400 nm to 700 nm for photosynthesis. An actinic light illuminated the whole plant through fibre optics and lens from above. The optical fibre exit is set as the whole plant can be uniformly illuminated. PPFs on the lowest and highest leaves were 130 and 160 μmol m^{-2} s^{-1}, respectively. Chlorophyll *a* fluorescence images were captured at 640 horizontal × 480 vertical pixels per flame with 8-bit (0–255) resolution from the above using a cooled charge-coupled device (CCD) camera (C5985, Hamamatsu Photonics, K.K., Japan) equipped with a band pass filter (MIF-W, central wavelength = 755 nm and half band width = 8 nm, Optical Coatings Japan Co., Ltd, Japan) and analysed by a computer.

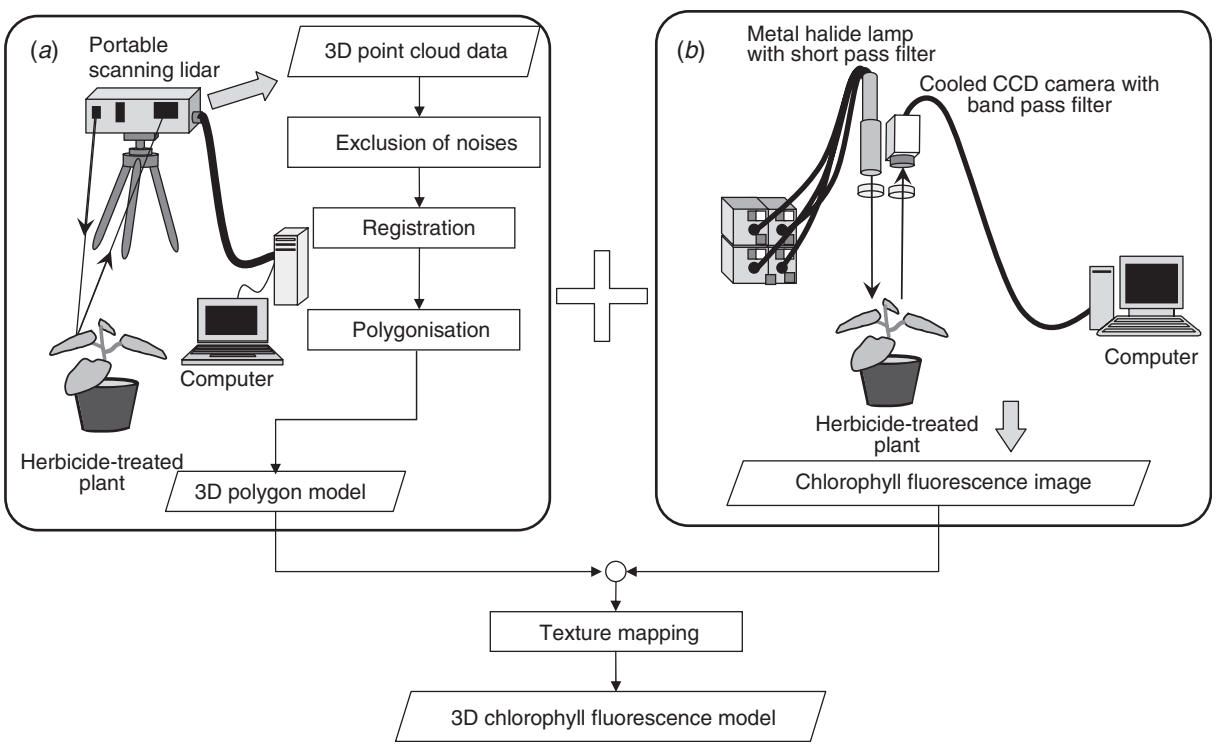

Fig. 1. (*a*) Combined range and (*b*) chlorophyll fluorescence imaging system and diagrammatic illustration of procedures for 3D chlorophyll fluorescence modelling of a whole plant. Procedure (*a*) represents the method of 3D lidar imaging. Procedure (*b*) represents the method of chlorophyll *a* fluorescence imaging. The images taken by the procedures (*a*) and (*b*) are combined by the texture-mapping technique.

Measurement and analysis of herbicide effects

After a whole plant was acclimated for 1 h under an actinic light, the steady-state chlorophyll *a* fluorescence image of all leaves of the plant was captured from one point above the plant (Fig. 1*b*). Thereafter, Nekosogi-ace water solution including the particles was poured into the soil around the roots in the pot. Chlorophyll *a* fluorescence images were intermittently captured at ~1/30 s every hour during a 5-h period after the herbicide treatment. Natural colour images were taken from different positions as JPEG image of 1600 horizontal × 1200 vertical pixels with a digital camera (Power Shot Pro1, Canon, Japan) just after the final chlorophyll fluorescence imaging. Spike-noises on the chlorophyll fluorescence images were eliminated by a median filter with the mask size of 3 × 3. 3D point cloud range data of the whole plant was measured with the lidar after the chlorophyll fluorescence measurements. The lidar measurements were conducted from four measuring points surrounding the plant to construct a complex 3D range image of all leaves without blind areas. The measurement time was a few minutes at each measuring point. The lidar data obtained from different measuring points were co-registered into the same orthogonal coordinates. Thereafter, the point cloud data was converted into a triangle-polygon image after noise exclusion, thus 3D range surfaces of leaves were expressed as irregular triangle meshes determined uniquely by arrangement of each point. Consequently, each leaf was created as a polygon shell in the 3D polygon model (3D range image). Laplacian smoothing was used to smooth polygon meshes.

A sequence of chlorophyll fluorescence images before and after the herbicide treatment and natural colour images taken after chlorophyll fluorescence measurements were mapped on the lidar-derived 3D polygon model of the whole plant by a texture-mapping technique (Heckbert 1986). The texture-mapping technique is widely applied as a method for adding surface texture to a computer-generated 3D polygon model. Digital 2D images like natural colour and chlorophyll fluorescence images are useable as the texture surface. Through the correspondence of the coordinates of 2D image to 3D polygon model, the information of 2D image is automatically mapped onto each polygon shell of the 3D polygon model. An accurate selection of the corresponding points between 2D and 3D images is of great importance to produce the complex texture mapping image of the plant. The corresponding points were then chosen from distinctive points on each leaf (e.g. the axils and edges). Subsequently, accurate 3D natural colour and 3D chlorophyll fluorescence models were constructed.

Leaf area was automatically calculated by summating areas of all polygons in each polygon shell, i.e. each leaf of 3D polygon model. The percentage of injured area, in which the chlorophyll fluorescence intensity exceeded the maximum value at each leaf site 1 h after the herbicide treatment, to whole area of each leaf was calculated from 3D chlorophyll fluorescence model. The mean value of leaf inclination and the standard deviation (s.d.) were obtained from 3D polygon model by averaging the values of 50 polygons selected randomly on the whole leaf.

Results

Three-dimensional natural colour model of a potted melon plant was produced by combining 2D natural colour images with a lidar-derived 3D polygon model. Different views of 3D natural colour model were shown in Fig. 2. The leaves from first (lowest) to fifth (highest) positions are indicated as numbers 1 to 5, in Fig. 2*a*, *b*, respectively. Circles, squares and triangles marked on the leaves in Fig. 2*a*, *b* correspond to the bases of each leaf. The produced models allowed 3D observation of shape, colour and texture of a whole plant from any points of view. All leaves inclined from the base to the tip, and especially the first and second leaves, which were older and looked somewhat more yellow than the other leaves, had steep slants. The visible injury was not observed in the 3D natural colour model at 5 h after the herbicide treatment.

Changes in 3D chlorophyll fluorescence intensity images from a 3D model view are shown in Fig. 3*a–f*, which correspond to before and at 1, 2, 3, 4 and 5 h after the herbicide treatment. Chlorophyll fluorescence intensity was uniformly distributed on all the leaves before the herbicide treatment (Fig. 3*a*). After herbicide treatment, increase in chlorophyll fluorescence intensity was observed slightly at the base of some leaves at 1 h (Fig. 3*b*). Increase in chlorophyll fluorescence intensity was also seen along main veins of leaves, except the fifth leaf, at 2 h (Fig. 3*c*). Thereafter, the increase gradually expanded to mesophylls of all leaves (Fig. 3*d–f*). The expansion was more significantly observed on the third and the fourth leaves than other leaves (Fig. 3*c–f*); however, it was least visible on the fifth leaf, at which the increase was hardly observed until 3 h after the herbicide treatment (Fig. 3*f*).

The earliest response site of chlorophyll fluorescence intensity is at the base of each leaf. Therefore, changes in chlorophyll fluorescence intensity were shown at leaf base sites marked in Fig. 2 after the herbicide treatment (Fig. 4). Before herbicide treatment, intensity of all sites was between 45 and 55 within an intensity range of 0 to 255 (8 bit). Changes in chlorophyll fluorescence intensity gradually appeared at the sites on the first to fourth leaves after 1 h of treatment. The intensity increases at the sites on third and fourth leaves were steeper than those at sites on the first and second leaves. The chlorophyll fluorescence intensity on third and fourth leaves reached around 160 at 5 h, while the first and second leaves were ~110 at 5 h. The intensity on the fifth leaf did not significantly change until 3 h, but increased to 95 at 5 h.

Differences in leaf area, leaf inclination and percentage of injured area to whole area of each leaf at 5 h after herbicide treatment were obtained from the 3D chlorophyll fluorescence model including the 3D polygon model (Fig. 5). The percentage of injured area distributed from 20.6 to 85.9%. The injuries of third and fourth leaves were very large and the percentages were 85.9% and 82.6%, respectively. The percentages of other leaves were below 50%, and especially those of the second and fifth leaves were 20.9% and 20.6%, respectively. The mean value of inclination from first to fifth leaves were 42.4 (s.d. = 15.1), 50.3 (16.7), 28.2 (12.2), 34.9 (7.3) and 28.5 (11.4) in degree, respectively. The first and second leaves had large inclination in comparison with the others. The leaf area ranged from 56 to 298 cm^2. The leaf areas of first, third and forth leaves were over 200 cm^2 but those of the second and fifth leaves were 127 $cm^2$and 56 cm^2, respectively. In particular, the fifth leaf was extremely small and immature. As shown in Fig. 6, there was a positive linear correlation ($R^2 = 0.72$, adjusted $R^2 = 0.63$, $P = 0.068$ in

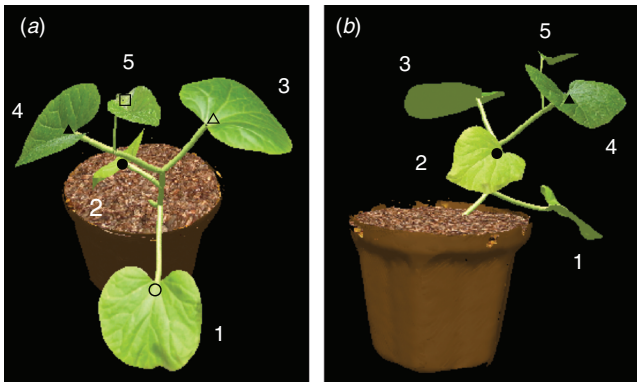

Fig. 2. Three-dimensional natural colour model of a melon (*Cucumis melo* L.) plant constructed by mapping natural colour images taken at 5 h after herbicide (Nekosogi-ace, including DCMU) treatment on the lidar-derived 3D polygon model. (*a*) and (*b*) are 3D images from different view points. The first to fifth leaves are indicated by the number 1 to 5. Open circle, filled circle, open triangle, filled triangle and open square marked on the leaves represent bases of first to fifth leaves.

F-test) between leaf area and percentage of injured area. For the relationship between leaf inclination and percentage of injured area, the value of fifth leaf were off from a negative linear correlation ($R^2 = 0.94$, adjusted $R^2 = 0.91$, $P = 0.031$ in *F*-test) among other leaves.

Discussion

A part of light energy absorbed by leaves is used for photosynthetic electron transport, and the residual energy is dissipated as heat and chlorophyll fluorescence emissions (Govindjee 2004). Herbicides affect the photosynthetic activities and leads to a change in the amount of dissipated energy. In the case of DCMU included in Nekosogi-ace, the effect on leaves appears as an increase in steady-state chlorophyll fluorescence intensity, where the primary l electron receptor Q_A of photosystem II is not reoxidated and thus photosynthetic electron transport is inhibited (Govindjee 2004). Therefore, the increase in chlorophyll fluorescence along the veins and the expansion to mesophylls were caused by DCMU transported with transpiration flow from the roots in the pot (Chaerle *et al*. 2003).

The affects of DCMU on chlorophyll fluorescence intensities were more significant at the third and fourth leaves than those of the first, second and fifth leaves (Figs 3, 4). It seems that the first and second leaves had already been senescent and the fifth leaf had still been immature seen as a slight yellow colour of the formers and insufficient leaf development of the latter (Figs 2, 5). That would have induced less stomatal opening and transpiration of the first, second or fifth leaves than those of the third and fourth leaves, thus the effects of DCMU would have been observed differently among leaves.

Transpiration flow rates at the base and veins of each leaf depend on whole leaf area and leaf conductance. Enlargements of leaf area and leaf conductance would increase transpiration flow rate and consequently DCMU transport and injury caused by the DCMU. The results of Fig. 6, especially the relationship between leaf area and percentage of injured area, support this assumption. Maximum stomatal conductance is strongly affected by growth conditions and changes with leaf age. In general, the maximum stomatal conductance of senescent and immature leaves becomes

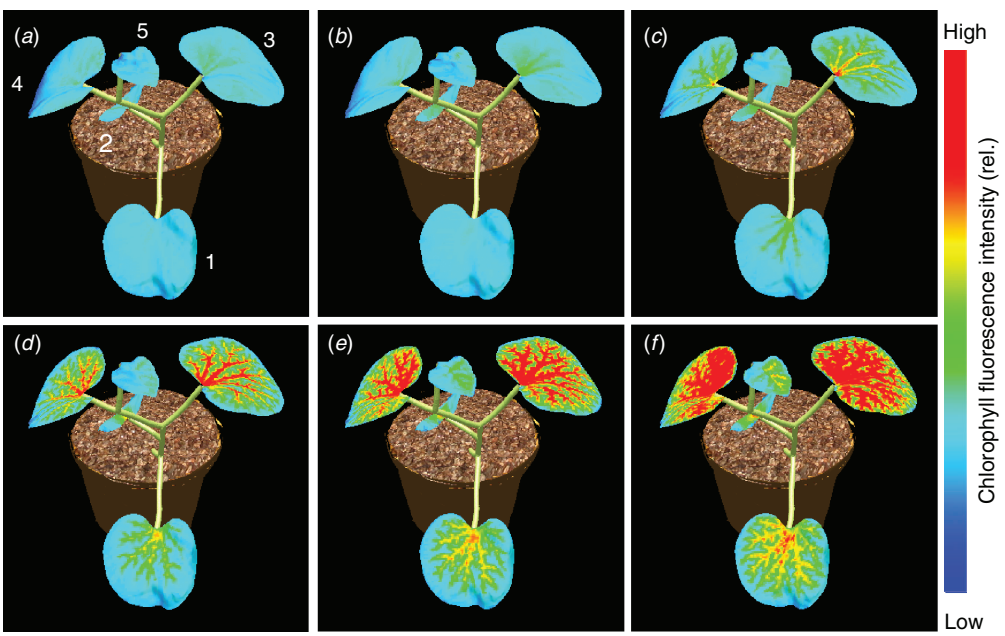

Fig. 3. Changes in 3D chlorophyll fluorescence intensity images from a view of the 3D model of the melon plant after the herbicide treatment. The plant is the same as shown in Fig. 2. (*a–f*) represent before and 1, 2, 3, 4 and 5 h after herbicide treatment. Numbers 1 to 5 in Fig. 3*a* correspond to the first to fifth leaves. The 3D model was constructed by combining the 2D chlorophyll fluorescence intensity images and the lidar-derived 3D polygon model.

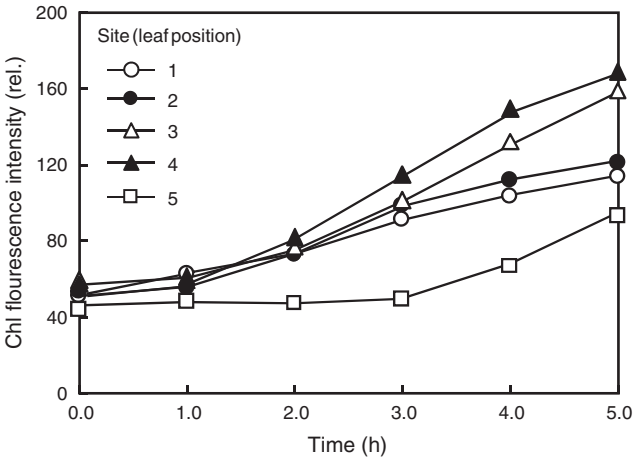

Fig. 4. Changes in chlorophyll fluorescence intensity at the bases of each melon leaf after the herbicide treatment. The sites of numbers 1 to 5 correspond to those in Fig. 2, respectively.

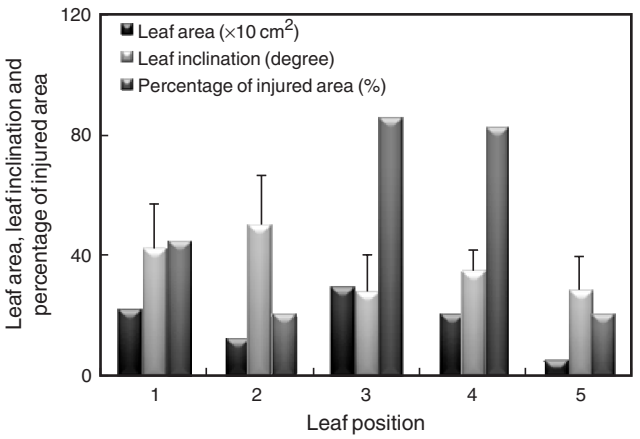

Fig. 5. Differences in leaf area, leaf inclination and percentage of injured area to whole area of each melon leaf 5 h after the herbicide treatment obtained from 3D chlorophyll fluorescence model (including 3D polygon model) shown in Fig. 3. The vertical bar of leaf inclination is the standard deviation (s.d.) of the values of 50 polygons selected randomly on the whole leaf.

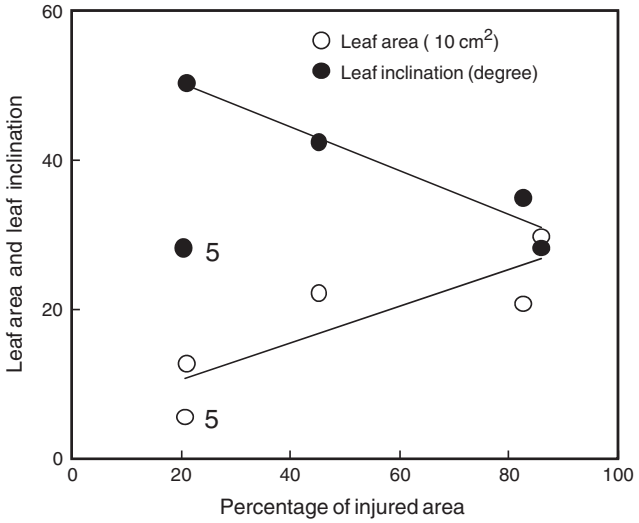

Fig. 6. Relationships between leaf area, leaf inclination and percentage of injured melon leaf area obtained from Fig. 5.

smaller than that of mature leaves (Jones 1983). Leaf shape and inclination change microenvironments such as light intensity and boundary layer conductance on the leaf (Ross 1981; Jones 1983; Sinoquet *et al*. 1998). Consequently, the stomatal conductance and the rates of transpiration flow and DCMU transport differ at each leaf site. In this experiment, the relationship between leaf inclination and percentage of injured area showed a negative linear correlation, except at the fifth, immature leaf (Fig. 6).

Steady-state chlorophyll fluorescence intensity increases with increasing actinic light intensity (Omasa *et al*. 1987). In this study, PPF of actinic light at the level on each leaf distributed between 130 and 160 $\mu mol\ m^{-2}\ s^{-1}$. The leaf inclination increased difference in PPF on the leaves. Consequently, the chlorophyll fluorescence intensity before the herbicide treatment varied between 44 and 59, and the difference was ~30%. Therefore, the percentage of injured area, in which the chlorophyll fluorescence intensity exceeded the maximum value at each leaf site during 1 h after the herbicide treatment, to whole area of each leaf was used as a more-steady index of the injury. Although this index was also affected by change in the leaf inclination during the experiment, the extent was very small because of little change in leaf inclination during the experiment.

It is difficult to measure accurately whole areas, injured areas, and site inclination of *in situ* curved leaves using ordinary 2D imaging. Therefore, 3D digitiser and stereo photogrammetry techniques (e.g. Lang 1973; Herbert 1995; Sinoquet *et al*. 1998) have been developed for estimations of leaf area and leaf inclination. Recent advances in computer technology and digital image sensors have made it possible to conduct more prompt 3D modelling and analysis for the plant structural parameters and growth responses (e.g. Ivanov *et al*. 1994; Omasa 2000; Andersen *et al*. 2005; Biskup *et al*. 2007; Omasa *et al*. 2007; Hosoi and Omasa 2009). Leaf fluctuations caused by wind during measurement affects accuracy of the 3D polygon model (Biskup *et al*. 2007). However, the affect on accuracy was very slight in the experiments (Fig. 2).

The present 3D chlorophyll fluorescence model allowed detection of spatio–temporal changes of physiological responses relating to photosynthetic electron transport of the herbicide on a whole plant, in addition to herbicide transport with transpiration flow from roots to leaves. Consequently, it was shown that the herbicide injury on the mature leaves was earlier and more severe than on the young and old leaves. The distance from veins, leaf area and leaf inclination influenced the extent of the injury within the leaves. These results indicate that differences in uptake of herbicide in the plant from soil depend on structural parameters of leaves and the microenvironments as well as leaf age. The findings should be verified by more detail studies on different growth stages and species. A possible advancement is to combine lidar-derived 3D polygon models with thermal and spectral reflectance images as well as chlorophyll fluorescence

images (Omasa *et al*. 2007). Therefore, the 3D composite imaging will increasingly improve our spatio–temporal understanding of biotic activities of plants and their responses to environmental stresses.

References

Andersen HJ, Reng L, Kirk K (2005) Geometric plant properties by relaxed stereo vision using simulated annealing. *Computers and Electronics in Agriculture* **49**, 219–232. doi: 10.1016/j.compag.2005.02.015

Biskup B, Scharr H, Shurr U, Rascher U (2007) A stereo imaging system for measuring structural parameters of plant canopies. *Plant, Cell & Environment* **30**, 1299–1308. doi: 10.1111/j.1365-3040.2007.01702.x

Campbell GS, Norman JM (1989) The description and measurement of plant canopy structure. In 'Plant canopies: their growth, form, and function'. (Eds G Russell, B Marshall, PG Jarvis) pp. 1–19. (Cambridge University Press: Cambridge)

Chaerle L, Hulsen K, Hermans C, Strasser RJ, Valcke R, Höfte M, Van der Straeten D (2003) Robotized time-lapse imaging to assess *in planta* uptake of phenylurea herbicides and their microbial degradation. *Physiologia Plantarum* **118**, 613–619. doi: 10.1034/j.1399-3054.2003.00143.x

Daley PF, Raschke K, Ball JT, Berry JA (1989) Topography of photosynthetic activity of leaves obtained from video images of chlorophyll fluorescence. *Plant Physiology* **90**, 1233–1238. doi: 10.1104/pp.90.4.1233

Endo R, Omasa K (2007) 3-D cell-level chlorophyll fluorescence imaging of ozone-injured sunflower leaves using a new passive light microscope system. *Journal of Experimental Botany* **58**, 765–772. doi: 10.1093/jxb/erl210

Genty B, Meyer S (1995) Quantitative mapping of leaf photosynthesis using chlorophyll fluorescence imaging. *Australian Journal of Plant Physiology* **22**, 277–284. doi: 10.1071/PP9950277

Govindjee (2004) Chlorophyll *a* fluorescence: a bit of basics and history. In 'Chlorophyll *a* fluorescence – a signature of photosynthesis'. (Eds GC Papageorgiou, Govindjee) pp. 1–42. (Springer: Dordrecht)

Govindjee, Nedbal L (2000) The chlorophyll fluorescence imaging and its application in plant science and technology. *Photosynthetica* **38**, 481–482. doi: 10.1023/A:1012485018944

Häder DP (2000) 'Image analysis: methods and applications.' 2nd edn. (CRC Press: Boca Raton, FL)

Heckbert PS (1986) Survey of texture mapping. *IEEE Computer Graphics and Applications* **6**, 56–67. doi: 10.1109/MCG.1986.276672

Herbert TJ (1995) Sterophotogrammetry of plant leaf angles. *Photogrammetric Engineering and Remote Sensing* **61**, 89–92.

Hosoi F, Omasa K (2009) Estimating vertical plant area density profile and growth parameters of a wheat canopy at different growth stages using three-dimensional portable lidar imaging. *ISPRS Journal of Photogrammetry and Remote Sensing* **64**, 151–158. doi: 10.1016/j.isprsjprs.2008.09.003

Ivanov N, Boissard P, Chapron M, Valéry P (1994) Estimation of the height and angles of orientation of the upper leaves in the maize canopy using stereovision. *Agronomie* **14**, 183–194. doi: 10.1051/agro:19940305

Jones HG (1983) 'Plants and microclimate: a quantitative approach to environmental plant physiology.' (Cambridge University Press: Cambridge)

Jones HG, Morison J (2007) Imaging stress responses in plants. *Journal of Experimental Botany* **58**, 743–898. doi: 10.1093/jxb/erl277

Lang ARG (1973) Leaf orientation of a cotton plant. *Agricultural Meteorology* **11**, 37–51. doi: 10.1016/0002-1571(73)90049-6

Omasa K (1990) Image instrumentation methods of plant analysis. In 'Modern methods of plant analysis'. (Eds HF Linskens, JF Jackson) pp. 203–243. (Springer-Verlag: Berlin)

Omasa K (2000) 3D color video microscopy of intact plants. In 'Image analysis: methods and applications'. 2nd edn. (Ed. DP Häder) pp. 257–273. (CRC Press: Boca Raton, FL)

Omasa K, Takayama K (2003) Simultaneous measurement of stomatal conductance, non-photochemical quenching, and photochemical yield of photosystem II in intact leaves by thermal and chlorophyll fluorescence imaging. *Plant & Cell Physiology* **44**, 1290–1300. doi: 10.1093/pcp/pcg165

Omasa K, Shimazaki K, Aiga I, Larcher W, Onoe M (1987) Image analysis of chlorophyll fluorescence transients for diagnosing the photosynthetic system of attached leaves. *Plant Physiology* **84**, 748–752. doi: 10.1104/pp.84.3.748

Omasa K, Saji H, Youssefian S, Kondo N (Eds) (2002) 'Air pollution and plant biotechnology.' (Springer-Verlag: Tokyo)

Omasa K, Hosoi F, Konishi A (2007) 3D lidar imaging for detecting and understanding plant responses and canopy structure. *Journal of Experimental Botany* **58**, 881–898. doi: 10.1093/jxb/erl142

Omasa K, Konishi A, Tamura H, Hosoi F (2009) 3D confocal laser scanning microscopy for the analysis of chlorophyll fluorescence parameters of chloroplasts in intact leaf tissues. *Plant & Cell Physiology* **50**, 90–105. doi: 10.1093/pcp/pcn174

Oxborough K (2004) Imaging of chlorophyll *a* fluorescence: theoretical and practical aspects of an emerging technique for monitoring of photosynthetic performance. *Journal of Experimental Botany* **55**, 1195–1205. doi: 10.1093/jxb/erh145

Oxborough K, Baker NR (1997) An instrument capable of imaging chlorophyll *a* fluorescence from intact leaves at very low irradiance and at cellular and subcellular levels of organization. *Plant, Cell & Environment* **20**, 1473–1483. doi: 10.1046/j.1365-3040.1997.d01-42.x

Rolfe SA, Scholes JD (2002) Extended depth-of-focus imaging of chlorophyll fluorescence from intact leaves. *Photosynthesis Research* **72**, 107–115. doi: 10.1023/A:1016053503453

Ross J (1981) 'The radiation regime and architecture of plant stands.' (Dr. W. Junk Publishers: The Hague)

Schurr U, Wakter A, Rascher U (2006) Functional dynamics of plant growth and photosynthesis – from steady state to dynamics – from homogeneity to heterogeneity. *Plant, Cell & Environment* **29**, 340–352. doi: 10.1111/j.1365-3040.2005.01490.x

Sinoquet H, Thanisawanyangkura S, Mabrouk H, Kasemsap P (1998) Characterization of the light environment in canopies using 3D digitizing image processing. *Annals of Botany* **82**, 203–212. doi: 10.1006/anbo.1998.0665

Manuscript received 12 May 2009, accepted 24 August 2009